PROCEEDINGS of the
23rd International Congress on Acoustics
9 to 13 September 2019 in Aachen, Germany

Sensitivity analysis for hybrid room acoustic simulation regarding spatial data of receiver

Philipp SCHÄFER, Michael VORLÄNDER

Institute of Technical Acoustics, RWTH Aachen, Germany, philipp.schaefer@akustik.rwth-aachen.de

Abstract

To overcome the limitations of methods using geometrical acoustics, Ray Tracing and Image Source algorithms can be combined with well-known numerical approaches - such as Finite Element Method (FEM) - which consider wave-based effects and therefore produce more sophisticated results in the lower frequency range. For this purpose, a room is modeled for both methods and then simulated separately. In a second step, the overall result can be received by uniting the distinct results in the frequency domain. A challenging aspect of room acoustic simulations is the acquisition of input data such as the receiver positions. The question arises how accurate this data has to be measured for the purpose of room acoustic simulations. Thus in the present work, a sensitivity analysis is conducted to determine the influence of deviations in the receiver position on the simulation result.

Keywords: Room Acoustics, Simulation, FEM, Ray Tracing, Image Sources

1 INTRODUCTION

The question of how the sound field in a room changes over space has been tackled in prior studies. Usually, the spatial fluctuation is investigated by comparing change of room acoustic single number quantities with the distance between two receiver points. Studies, such as by Witew et al. [6], are based on simulation methods using approaches from geometrical acoustics. Thus, in the present work a hybrid approach combining the strength of geometric and wave-based simulations is made. This paper focuses on the low to medium frequency range where wave-based effects like room modes are considered. For this purpose, investigations of the spatial deviation of reverberation time T_{30} in a reverberation chamber are carried out. In this context, it is also investigated whether these deviations have a directional component.

2 HYBRID WAVE-BASED AND GEOMETRICAL ACOUSTIC SIMULATION TOOL

When combining wave-based and geometric acoustic (GA) methods for room acoustic simulations, two models have to be designed. The models should be equivalent in their geometric and acoustic properties. Furthermore, the simulation settings have to be adjusted to the considered problem. Afterwards, both simulations can be carried out independently. Both results are then combined using a cross-fade filter in the frequency domain [3]. Since the wave-based result is usually band-limited, the crossover frequency should be in an adequate distance below the upper cut-off frequency. The overall procedure of this simulation approach is illustrated in figure 1. More details on the distinct simulation methods are given in the following sections.

2.1 FE simulation via COMSOL

For the calculation of the low frequency range room transfer function, the well-known finite element method (FEM) is utilized. This method allows to numerically solve the Helmholtz wave equation giving a volume mesh of the considered room. As additional input, the boundary and source conditions have to be specified using impedances and velocities. This method allows to evaluate the sound pressure at each point within the room using a single simulation. In this work, all simulations are carried out using COMSOL Multiphysics 5.4 [1] including the Acoustics Module.

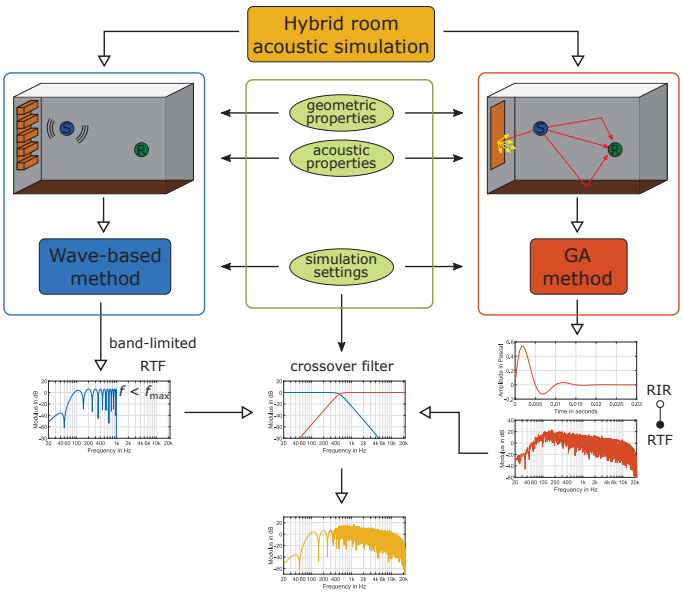

Figure 1. Block diagram of hybrid wave-based and geometrical acoustic simulation.

2.2 RAVEN

The geometrical acoustic simulation tool RAVEN [5] uses a hybrid approach of image sources and stochastic ray tracing. Giving an simple surface model of the considered room, it allows to predict the room impulse response (RIR) of specified source-receiver pairs. The boundary conditions are modeled using the frequency-dependent absorption and scattering coefficients α and s. Although the sources are considered to be points, arbitrary sources can be modeled using a directivity and free field sensitivity. On the other hand, the receiver is modeled as point for the image source method but as sphere for the ray tracing method.

3 SIMULATION SCENARIOS

The scenarios considered in this research take place in the reverberation chamber at ITA of RWTH Aachen. They are based on a former investigation of Pelzer et al. [4]. Of the three suggested boundary condition scenarios, only the first two are considered here - the empty reverberation chamber and a scenario with mineral wool at two of the walls (see [4], section 3, scenario a) and b)). Both scenarios are shown in figure 2. A single source is used to excite the room. Since only mono RIRs are considered in this work, all receivers are modeled as omnidirectional. Thus, no further geometries (such as a dummy head) are added to the FE room model. In the following, the two considered scenarios are referred to as

- Empty room
- Absorber wall

3.1 Boundary conditions

The boundary conditions are the only parameters that are varied between the simulation scenarios. There are two materials considered here: The reverberant wall of the room and a mineral wool that acts as absorber. Their acoustic parameters - specific impedance, absorption coefficient and scattering coefficient - are shown in figure 3. The data is taken from [4]. While in scenario "Empty room" only the first material is used, in scenario "Absorber wall", the mineral wool is applied to two walls (see fig. 2).

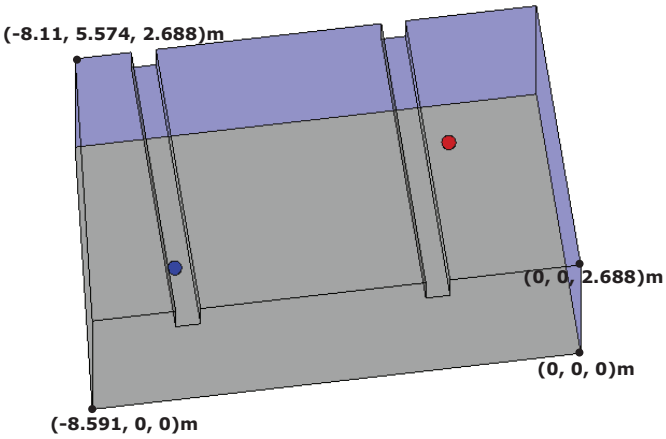

Figure 2. Room model of the reverberation chamber at ITA of RWTH Aachen. The source position is marked as blue, the center position of the receiver grid as red circles. For the scenario "Absorber wall", the mineral wool is applied to the two walls highlighted in light blue. The room has a rectangular shape except for the left wall which is placed in an angle greater than 90° and two beams at the ceiling.

3.2 Source model

A single source is used to excite the room. Although compared to [4] the source position is unchanged at $(-6.902, 1.714, 1.543)\,\mathrm{m}$, it is modeled as perfect monopole with a flat frequency response for both simulation methods. Thus, no directivity is applied to the GA source model.

3.3 Receiver positions

In context to the research question, multiple receivers are placed in form of a grid for the simulation. The grid has a resolution of 1 cm in x-, y- and z-direction respectively and is centered at $(-1.817, 3.591, 1.696)\,\mathrm{m}$. It spans from $-5\,\mathrm{cm}$ to $+5\,\mathrm{cm}$ in each direction around the center leading to a total number of receivers of

$$N_{\mathrm{grid}} = 11^3 = 1331. \tag{1}$$

3.4 Simulation settings

The simulation settings are summarized in table 1. It is important to mention that the crossover frequency roughly corresponds to the Schroeder frequency of the considered room. Furthermore, a highpass filter (butterworth, order 8) is applied to the FE results to remove potential zero order modes.

Table 1. Simulation settings

COMSOL	
Simulation frequencies	0.1 Hz : 0.1 Hz : 400 Hz
Highpass filter	$f_{\mathrm{cutoff}} = 10\,\mathrm{Hz}$
Mesh frequency (5 elements per wavelength)	340 Hz

RAVEN	
Image source order	4
Radius of receiver sphere	0.2 m
Number of rays (per frequency band)	100,000

Combination filter	
Crossover frequency	340 Hz
Filter type	Butterworth
Filter order	16

Ambient settings	
Static pressure	101000 Pa
Temperature	291.35 K (18.2°C)
Relative humidity	43 %

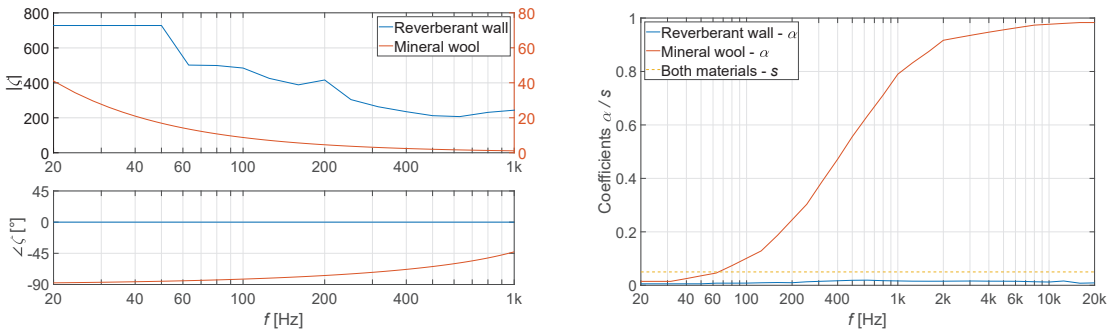

(a) Specific impedance

(b) Absorption and scattering coefficient

Figure 3. Acoustic boundary conditions of the two utilized materials according to [4]. Note that the specific impedance magnitude of the mineral wool is plotted using a scale of factor 10 (right y-axis). Furthermore, the specific impedance for the reverberant wall is real-valued and calculated from the corresponding absorption coefficient. The scattering coefficient is assumed to be 5 % for both materials at all frequencies.

4 RESULTS

For each scenario and each receiver position, a combined broadband room impulse response is simulated. Exemplarily, the room transfer functions at the grid's center position are shown in figure 4. To compare the results

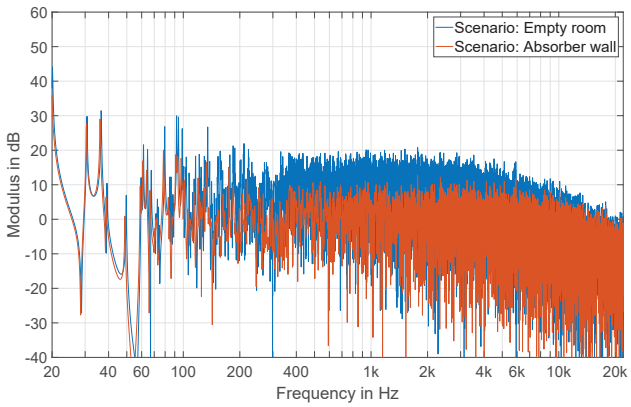

Figure 4. Room transfer functions for both scenarios evaluated at the center position of the receiver grid.

between different receiver positions, single value room acoustic parameters can be utilized [6]. The reverberation time is one of the most frequently used room acoustic parameters. Especially, in the context of absorption coefficient measurements in reverberation chambers it is of special interest. Thus, the reverberation time T_{30} is calculated for each RIR according to [2] for third-octave bands. No noise compensation is used, since the noise floor of the simulation results is expected to be very low (numerical noise only).

4.1 Statistical spreading over receiver grid

In order to get an impression of how the reverberation time changes over the receiver grid volume, the relative deviation is calculated for each point. As a reference, the mean value over all grid points $\boldsymbol{r}_i$

$$T_{\text{mean}} = \frac{\sum_i^{N_{\text{grid}}} T(\boldsymbol{r}_i)}{N_{\text{grid}}} \tag{2}$$

is used. Then, the relative deviation at observation point $\boldsymbol{r}$ becomes

$$\eta_T(\boldsymbol{r}) = \frac{|(T(\boldsymbol{r}) - T_{\text{mean}})|}{T_{\text{mean}}}. \tag{3}$$

The results are shown in the boxplots in figure 5. Note that the minimum frequency is limited to 80 Hz due

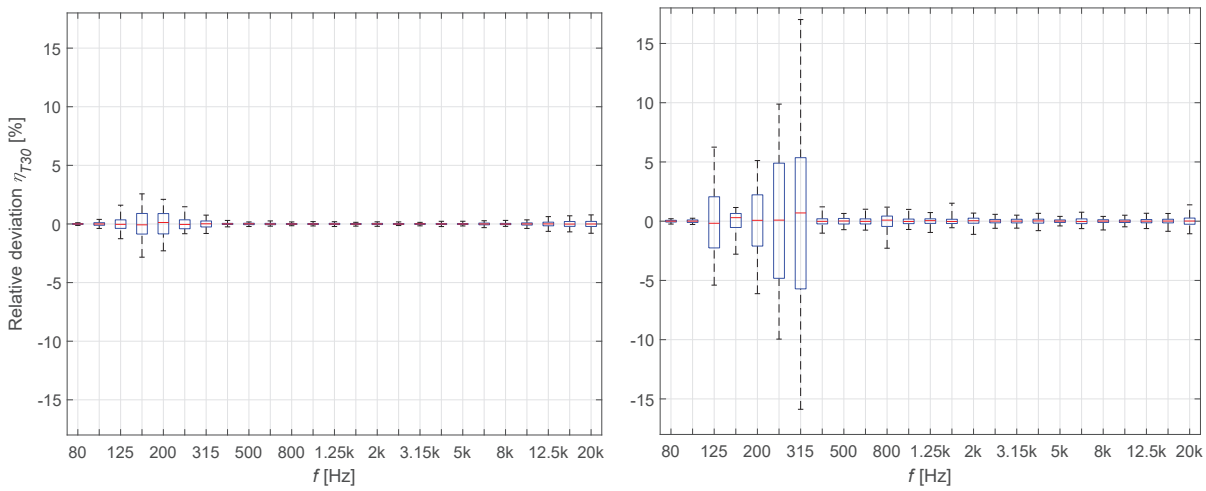

(a) Scenario: Empty room

(b) Scenario: Absorber wall

Figure 5. Boxplots of relative deviation of reverberation time over the receiver grid for both scenarios and third octave bands. The maximum whisker size is set to four times the interquartile range.

to the maximum length of the RIRs ($t_{\max} = \frac{1}{\Delta f} = 10\,\text{s}$) and the high reverberation time of the room at low frequencies ($T \gg 10\,\text{s}$). As expected, η_T is very small at frequencies below 125 Hz where the wavelength is much larger than the receiver grid. Furthermore, it can be observed that the statistical spreading is higher for the scenario "Absorber wall". For both scenarios, η_T has the highest variance in the lower frequency bands around approximately 200 Hz where the result is based on the FE simulation. Above the crossfade frequency of 340 Hz the deviation is much smaller. Only in scenario "Empty room" for $f \geq 10\,\text{kHz}$ an increase of η_T is observed again which is most likely caused by the effect of air absorption. A visual inspection of the EDCs of the lower frequency bands shows that the energy decay is not strictly exponential but shows ripples (not shown for brevity). Thus, the observed deviations might be caused by a non smooth decay process. Also for scenario "Absorber wall", there is a mismatch in the variance at the crossover between the FE and GA results. This suggests that in this frequency range, wave-based effects are not negligible and therefore the GA approach is not sufficient. In the following section, further investigations are conducted for the FE frequency bands.

4.2 Distance between receiver points

In order to set the deviation of the reverberation time in relation to the distance between observation points, additional parameters are introduced. Assuming two receiver positions $\boldsymbol{r}_n$ and $\boldsymbol{r}_m$ and the vector

$$\Delta\boldsymbol{r} = \boldsymbol{r}_n - \boldsymbol{r}_m = \begin{pmatrix} \Delta r_x & \Delta r_y & \Delta r_z \end{pmatrix}^{\mathsf{T}} \tag{4}$$

connecting them, then the spatial three-dimensional distance between both receiver points can be expressed taking the absolute value of each component:

$$\boldsymbol{d} = \begin{pmatrix} d_x \\ d_y \\ d_z \end{pmatrix} = \begin{pmatrix} |\Delta r_x| \\ |\Delta r_y| \\ |\Delta r_z| \end{pmatrix} \tag{5}$$

On the other hand, the absolute inter-receiver distance is calculated by applying the l^2-norm:

$$d = \|\boldsymbol{d}\| = \|\Delta\boldsymbol{r}\| = \sqrt{\Delta r_x^2 + \Delta r_y^2 + \Delta r_z^2} \tag{6}$$

Regarding the simulated reverberation times, the absolute deviation between these two observation points is

$$\Delta T(\boldsymbol{r}_n, \boldsymbol{r}_m) = |T(\boldsymbol{r}_n) - T(\boldsymbol{r}_m)|\,. \tag{7}$$

The relative deviation is derived normalizing eq. 7 to the mean reverberation time of the receiver grid (eq. 2):

$$\eta_T(\boldsymbol{r}_n, \boldsymbol{r}_m) = \frac{\Delta T(\boldsymbol{r}_n, \boldsymbol{r}_m)}{T_{\text{mean}}}. \tag{8}$$

For the investigation in the following two sections, eq. 8, 5 and 6 are evaluated for all receiver pairs along the receiver grid resulting in

$$N_{\text{data}} = N_{\text{grid}} \cdot \frac{N_{\text{grid}} - 1}{2} = 885115 \tag{9}$$

data pairs of d and η_T or $\boldsymbol{d}$ and η_T respectively. It is important to mention, that N_{data} exceeds the number of possible inter-receiver distances. Thus, values of η_T referring to the same distance d or $\boldsymbol{d}$ are summarized using a respective mean operation:

$$\eta_T(d_n) = \overline{\eta_T(d_i = d_n)} \tag{10}$$

$$\eta_T(\boldsymbol{d}_n) = \overline{\eta_T(\boldsymbol{d}_i = \boldsymbol{d}_n)} \tag{11}$$

4.3 Evaluation of absolute distance

In this section, the influence of the absolute distance between two observation points on the reverberation time is investigated. For this purpose, the relative deviation of the reverberation time is evaluated according to section 4.2 and processed according to eq. 10. Note that at high distances ($d > 0.14$), the number of data samples used for the average is very small (e.g. there are only four receiver pairs with $d = d_{\max} = \sqrt{3} \cdot 0.1\,\text{m}$). The results for both scenarios are shown in figure 6. As expected, η_T grows with increasing inter-receiver distance.

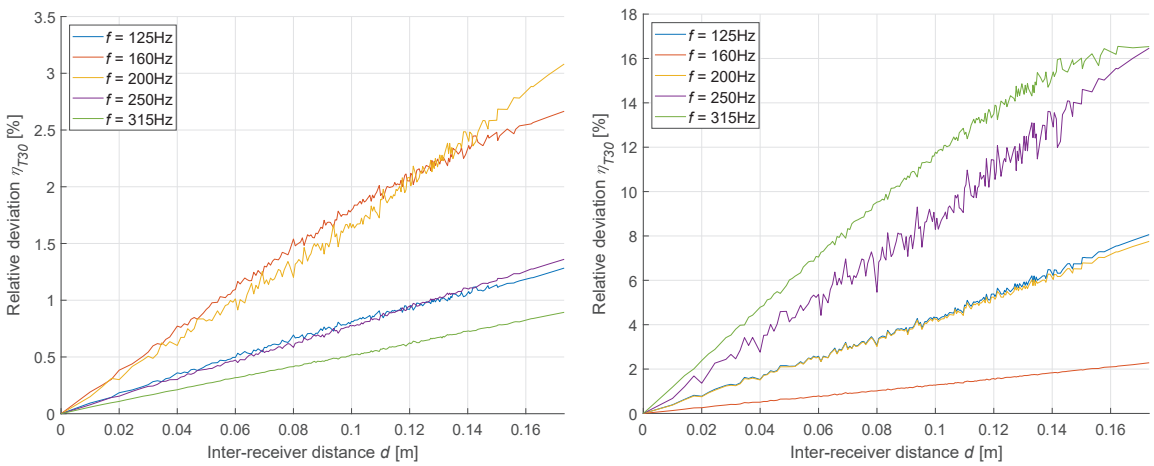

(a) Scenario: Empty room

(b) Scenario: Absorber wall

Figure 6. For both scenarios, the relative deviation in the reverberation time η_T is shown as function of the absolute inter-receiver distance d. Values that refer to the same distance are summarized using eq. 10.

Furthermore, there are large differences between the considered frequencies. This is likely to be caused by modal effects. For most frequencies, the scenario "Absorber wall" has a higher deviation in reverberation time than the scenario "Empty room". At 250 Hz and 315 Hz, it is even above 15 %. Due to the absorber material on two of the walls, the sound field is less diffuse. Thus, a higher fluctuation of the reverberation time over space is expected. η_T might also be increased since the receiver grid is placed very close to the absorber walls.

4.4 Evaluation of 3D-distance

Now, an investigation similar to the previous section is done regarding the three-dimensional distance $\boldsymbol{d}$. Therefore, the reverberation time data $\eta_T(\boldsymbol{d})$ is processed according to eq. 11. The results are shown in multiple

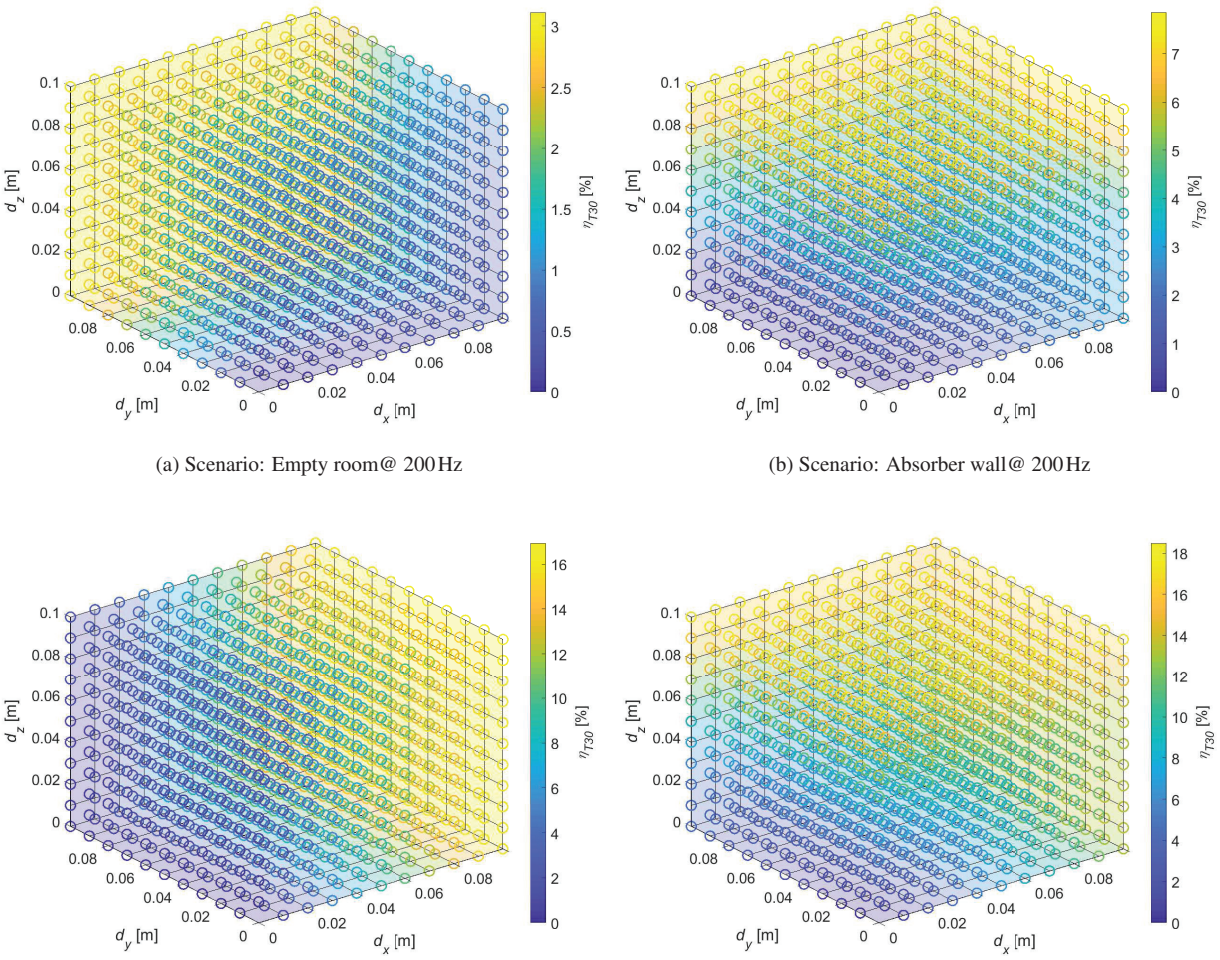

(a) Scenario: Empty room@ 200 Hz

(b) Scenario: Absorber wall@ 200 Hz

(c) Scenario: Absorber wall@ 250 Hz

(d) Scenario: Absorber wall@ 315 Hz

Figure 7. Scatter plot of the relative deviation of reverberation time η_T as function of the inter-receiver distance vector d_x, d_y and d_z. Values that refer to the same distance vector are summarized using eq. 11.

scatter plots in figure 7. For the considered frequencies, it can be seen that η_T not only depends on the inter-receiver distance, but also on its directional components d_x, d_y and d_z. The differences between the directions

can be large. For example at 250 Hz in the "Absorber wall" scenario, the deviation at $d_x = 0.1$ m can be up to 16 % whereas at $d_x = 0$ m it is below 1 %. In this case, d_x seems to be the "dominant" direction for the change of the reverberation time. Comparing the three results for scenario "Absorber wall", this direction also seems to change with frequency. Furthermore, it seems to be influenced by the boundary conditions as can be seen comparing the results at 200 Hz. Additional investigations are necessary to check whether this phenomenon can be reproduced in further simulation scenarios.

5 CONCLUSIONS

In the course of this work, it could be shown that for the considered scenarios the reverberation time T_{30} calculated from hybrid room acoustic simulations significantly deviates over a small receiver grid. The high fluctuation can be observed in the frequency bands just below the Schroeder frequency where the results are based on the FE tool.

In the scenario with absorber around the crossfade frequency of 340 Hz, a mismatch in the variance of the relative deviation of T_{30} between the FE and GA results could be observed. Here, the approximation of geometric acoustics might not be valid due to the strong difference of the absorption coefficients of the walls. Thus, the FE simulation should be extended to higher in future studies in order to validate this.

It could be shown that in average, the relative deviation of T_{30} increases with the distance between two observation points. Also for the frequency bands around 200 Hz, this spatial deviation seems to be directional. Depending on the considered frequency and the boundary conditions, the deviation towards one direction (x, y or z) is greater than towards the others. As expected, this phenomenon is more prominent in the scenario with absorber.

The findings of this study suggest that - depending on the considered frequency range, the room geometry and boundary conditions - the FE results of a hybrid room acoustic simulation might vary significantly even for small changes in the receiver position due to modal effects. Additional investigations have to be done to evaluate this. In this context, a variation of the receiver grid position and size is of interest. Most importantly, the spatial deviation of additional room acoustic parameters should be investigated.

REFERENCES

[1] COMSOL Multiphysics® 5.4, COMSOL AB, Stockholm, Sweden. www.comsol.com.

[2] ISO EN DIN 3382-1, Measurement of room acoustic parameters - Part 1: Performance spaces. *International Organization for Standardization, Brussels, Belgium*, 2009.

[3] M. Aretz. *Combined wave and ray based room acoustic simulations of small rooms*. Doctoral dissertation, RWTH Aachen University, Germany, 2012.

[4] S. Pelzer, M. Aretz, and M. Vorländer. Quality assessment of room acoustic simulation tools by comparing binaural measurements and simulations in an optimized test scenario. *Proceedings of Forum Acusticum*, 2011.

[5] D. Schröder. *Physically based real-time auralization of interactive virtual environments*. Doctoral dissertation, RWTH Aachen University, Germany, 2011.

[6] I. Witew, P. Dietrich, S. Pelzer, and M. Vorländer. Comparison of different modelling strategies to predict the spatial fluctuation of room acoustic single number quantities. In *40th Italian (AIA) Annual Conference on Acoustics and the 39th German Annual Conference on Acoustics (DAGA)*, 2013.